

Article

# The Potential of High-Fluence Ion Irradiation for Processing and Recovery of Diamond Tools

Anatoly M. Borisov <sup>1,2,\*</sup>, Valery A. Kazakov <sup>3</sup>, Eugenia S. Mashkova <sup>4</sup>,  
Mikhail A. Ovchinnikov <sup>4</sup> , Sergey N. Grigoriev <sup>2</sup>  and Igor V. Suminov <sup>2</sup>

<sup>1</sup> Moscow Aviation Institute (National Research University), 125993 Moscow, Russia

<sup>2</sup> Moscow State Technological University “STANKIN”, 127994 Moscow, Russia;  
s.grigoriev@stankin.ru (S.N.G.); ist3@mail.ru (I.V.S.)

<sup>3</sup> Chuvash State University, 428015 Cheboksary, Russia; cossac@mail.ru

<sup>4</sup> Skobeltsyn Institute of Nuclear Physics, Moscow State University, 119991 Moscow, Russia;  
es\_mashkova@mail.ru (E.S.M.); ov.mikhail@gmail.com (M.A.O.)

\* Correspondence: anatoly\_borisov@mail.ru

Received: 26 November 2020; Accepted: 15 December 2020; Published: 17 December 2020



**Abstract:** The graphitization and surface growth of synthetic diamonds by high-fluence irradiation with 30 keV argon and carbon ions have been experimentally studied. Scanning electron microscope (SEM) and atomic force microscope (AFM) show removal of traces of mechanical polishing. The ion-induced roughness does not exceed 20 nm. Raman spectroscopy and the measurement of electrical conductivity confirm the graphitization of the surface layer when irradiated with argon ions at the temperature of 230 °C and the diamond structure of the synthesized layer when irradiated with carbon ions at the temperature of 650 °C.

**Keywords:** monocrystalline; high-pressure, high-temperature (HPHT) diamond; chemical vapor deposition (CVD) diamond; high-fluence ion irradiation; Ar<sup>+</sup>; C<sup>+</sup>; SEM; AFM; Raman spectra; electrical conductivity

## 1. Introduction

Ionic and neutral atomic and molecular beams are very promising for the synthesis of tool-hardening coatings on an industrial scale [1–9]. Diamond is widely used as an abrasive, as an indenter and cutting tool, and as a heat sink in electronic devices, including as a filler in composite highly heat-conducting materials, and its use in microelectronics is promising. Among the methods for obtaining synthetic diamonds and diamond-like coatings, the method of the ion implantation of carbon has certain advantages. According to [10], the ion implantation of carbon into natural diamond crystals leads to internal epitaxial growth without a visible interface between the grown layer and the crystal surface. The layer synthesized by ion implantation has the same high resistance to acids and oxidation in air at 500 °C as natural diamond. Neither one is polished with aluminum oxide; both behave the same when lapping on a diamond polishing wheel and when scratching with a diamond needle or a diamond indenter.

The influence of high-fluence ion irradiation by 10–30 keV Ar<sup>+</sup>, Ne<sup>+</sup>, N<sup>+</sup>, N<sub>2</sub><sup>+</sup> and C<sup>+</sup> ions at temperatures from 30 to 720 °C on the conductivity and microstructure of a polycrystalline diamond surface layer was experimentally studied in [11,12]. The increase in diamond temperature during irradiation leads to ion-induced graphitization at  $T_{ir} > T_{gr} \approx 200$  °C. The Raman spectra indicate that irradiation with neon and argon ions at temperatures of the diamond more than  $T_{ir} > 500$  °C leads to the formation of a nanocrystalline graphite layer that increases the resistivity of the irradiated layer. This effect is not observed under irradiation by nitrogen ions. It was found that dynamic annealing at

temperatures above 500 °C leads to the recrystallization of the diamond only in the case of irradiation with carbon ions, and irradiation with impurity ions causes graphitization of the ion-modified diamond layer. Under irradiation with carbon ions, the growth and recrystallization of diamond with a thin (~1 nm) graphite-like layer on the surface occurs.

For the processing and restoration of diamond tools, there is an interest in determining the conditions for the graphitization of the diamond surface to a given thickness and controlled surface growth. A soft graphitized layer on the surface of a diamond can facilitate its mechanical polishing and can be used as a sacrificial layer for planarization. There is an interest in surface build-up for resizing and reshaping a unique diamond tool. In both cases, it is important to reduce or at least maintain the surface roughness during processing.

In this work, graphitization with argon ions, which begins at a temperature of >230 °C, and the growth of diamond under irradiation with carbon ions at a temperature of >500 °C were chosen as the most promising for instrumental application. The effect of high-fluence ion irradiation on the surface morphology was studied by SEM and AFM methods, and the structure of the irradiated layer was studied by Raman spectroscopy and electrical conductivity measurements.

## 2. Materials and Methods

Samples of synthetic polycrystalline diamond and single crystal Ib diamond were used. A 450 µm-thick polycrystalline diamond plate was prepared by chemical vapor deposition on a silicon substrate 63 mm in diameter [13,14]. A (111) face diamond crystal was obtained by high-pressure, high-temperature growth in Fe–Ni–C liquid from the seed [15,16]. High-fluence irradiation with Ar<sup>+</sup> and C<sup>+</sup> ions was carried out along the normal to the sample surface on a mass monochromator of the Skobeltsyn Institute of Nuclear Physics, Moscow State University [17]. The ion energy was 30 keV. The ion current density reached 0.4 mA/cm<sup>2</sup> at a beam cross section of 0.3 cm<sup>2</sup>. The irradiation fluences  $\varphi t$  ( $\varphi$  = the ion flux density, and  $t$  = the irradiation time) were no less than 10<sup>18</sup> ions/cm<sup>2</sup> for all the cases of diamond irradiation. The flat resistive furnace in the target holder allows heating the target up to 720 °C. The target temperature was measured with a chromel alumel thermocouple fixed on the irradiated side of the sample outside of the irradiation area. Samples irradiated at  $T = 30$  °C were isochronally annealed in a vacuum with a one-hour thermal treatment as the maximum cycle temperature  $T$  was increased sequentially from 100 to 720 °C.

The modified target was examined by SEM with a Lyra 3 (TESCAN, Brno, Czech Republic), AFM with a Dimension V (Veeco, Plainview, NY, USA) and a T64000 Raman spectrometer (Horiba Jobin Yvon, Edison, NJ, USA). Laser radiation with a wavelength of 488 nm for a single diamond crystal and a wavelength of 514 nm for a polycrystalline diamond was used to excite Raman scattering. Electrical measurements of the sheet resistance  $R_s$  were used in a four-point probe method at room temperature.

## 3. Results and Discussion

### 3.1. Characterization of High-Fluence Ion Irradiation

For the characterization of high-fluence ion irradiation, the depth distributions  $\nu(x)$  of the numbers of displacements per atom (dpa) (damage depth profiles) were calculated. The profiles  $\nu(x)$  were determined by the depth distributions  $\Sigma(x)$  of the average numbers of vacancies formed by one ion per path length, which were derived by the computer simulation of the ion interactions with solids using the SRIM code [18]. At not-too-high fluences  $\nu(x) \approx \Phi \cdot \Sigma(x)/n_0$ , where the fluence  $\Phi = \varphi \cdot \tau$  is equal to the product of the ion beam flux  $\varphi$  and irradiation time  $\tau$ ,  $n_0$  is the atomic target concentration [19]. At high fluences, dynamic equilibrium conditions are established, in which the profiles of the concentration

of implanted particles and radiation damage become stationary [11]. The stationary damage depth profile  $\nu_{st}(x)$  is calculated as follows:

$$\nu_{st}(x) = \frac{1}{K} \int_x^{R_d} \Sigma(x') \cdot dx', \quad (1)$$

where  $R_d$  is the depth of the defect production,  $K = Y$  for  $\text{Ar}^+$  ion irradiation,  $K = |1-Y|$  for  $\text{C}^+$  ion irradiation and  $Y$  is the sputtering yield.

The calculated stationary profiles  $\nu_{st}(x)$  are shown in Figure 1. Based on the calculated profiles of  $\nu_{st}(x)$ , the thickness  $t$  of the modified surface layer was estimated.

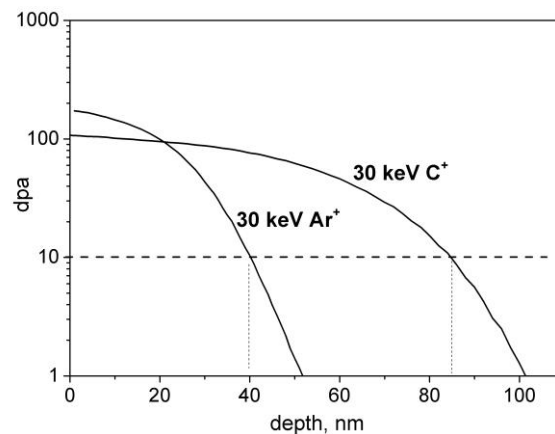
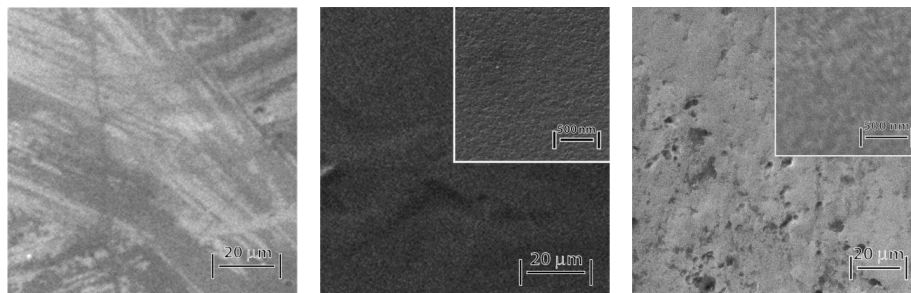


**Figure 1.** Stationary damage depth profiles under high-fluence ion irradiation.

The value of  $t$  was determined from the level of 10 dpa. This value of  $\nu$  was attained over the depths  $x \leq R_d$ . Unlike for irradiation by gas ions, for  $\text{C}^+$  ion irradiation, the thickness of the modified layer increases due to the implanted carbon ions, since the self-sputtering yield ( $Y = 0.21$ ) is less than 1 [20]. For estimating the thickness  $t$ , the thickness of the deposited carbon was added to the modified layer thickness obtained from  $\nu_{st}(x)$ .

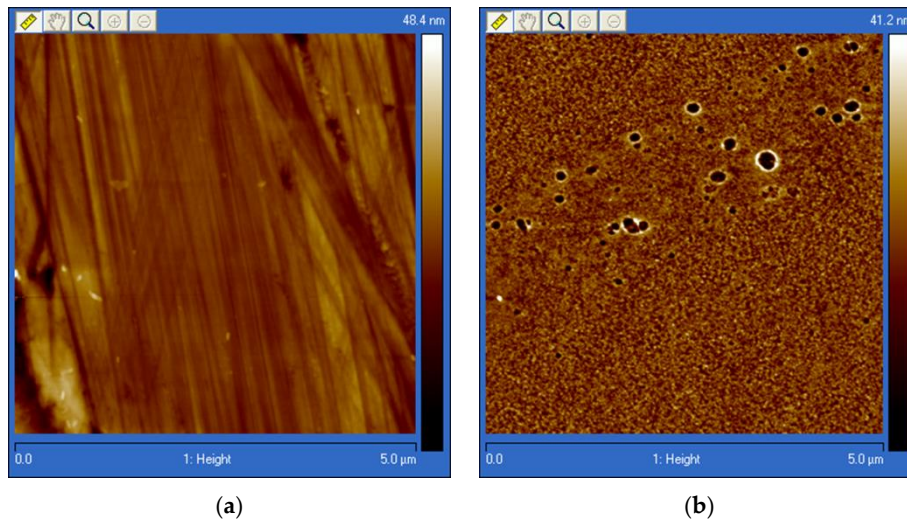
### 3.2. SEM and AFM

Figure 2 shows SEM images of the (111) face of the diamond before and after irradiation with argon and carbon ions at temperatures of 230 and 650 °C, respectively. The radiation fluences in both cases were equal to  $1.3 \times 10^{18}$  ion/cm<sup>2</sup>. Traces of mechanical polishing are clearly visible on the surface before irradiation, which were removed by high-fluence ion irradiation. At the same time, the ion irradiation led to the appearance of etching pits in the form of equilateral triangles with sides of about 20  $\mu\text{m}$  and open micropores. Such micropores are associated, as a rule, with the increased sputtering of areas of clusters of crystal structure defects, which lower the binding energy of surface atoms. At higher magnification, a stochastic nanoglobular relief appears in the SEM images (insets in Figure 2).



**Figure 2.** SEM images of the (111) face of the diamond: (a) before irradiation, (b) after irradiation with 30 keV  $\text{Ar}^+$  230 °C ions and (c) after irradiation with 30 keV  $\text{C}^+$  650 °C ions.

The AFM measurements of the relief also show the removal of the traces of mechanical polishing under ion irradiation and the appearance of a stochastic nanorelief (Figure 3). The roughnesses before and after the irradiation of the diamond surface are close; the root-mean-square roughness at a base length of 1  $\mu\text{m}$  is about 20 nm.



**Figure 3.** AFM images of the (111) face of diamond (a) before irradiation and (b) after  $\text{Ar}^+$  ion irradiation with 30 keV at  $T = 230$  °C.

It should be noted that the described results for the ion-beam treatment of the diamond surface are not common. The high-fluence ion irradiation of most metals and semiconductors leads to a significant development of ordered (in the form of ripples) and stochastic reliefs (in the form of cones, pyramids, ridges, etc.). The ion irradiation of graphite-like carbons also leads to a significant development of the relief. In particular, the irradiation of highly oriented pyrographite, which is the closest in structure to a single crystal of graphite, leads to an extreme development of microrelief in the form of sharp ridges of micron size in a temperature range for the irradiated samples from room temperature to 400 °C [21]. Such a strong effect of the temperature of the irradiated diamond samples on the ion-induced relief was not observed. In particular, the ion-induced relief after irradiation with argon ions with an energy of 30 keV at temperatures of 230 and 400 °C is practically the same [22].

### 3.3. Raman Spectroscopy

It is known that Raman spectroscopy (RS) is an effective method for studying carbon materials [23]. In RS spectra in the frequency range  $1000\text{--}1700\text{ cm}^{-1}$ , diamond gives a single narrow peak at  $1332\text{ cm}^{-1}$ , and graphite-like materials manifest themselves as characteristic D and G peaks, with frequencies for microcrystalline graphite of  $1345$  and  $1580\text{ cm}^{-1}$ , respectively. The Raman spectra of graphite-like materials can also contain peaks at the frequencies  $1200$ ,  $1500$  and  $1620\text{ cm}^{-1}$ . These peaks appear for disordered or nanocrystalline graphite-like materials and are associated with the disorder of the planar structure of crystallites, boundary scattering when crystallites are reduced to nanometer sizes, disorder of translational symmetry, ionic impurities in materials and formation of carbyne chain compounds.

Raman spectroscopy data obtained after the ion irradiation of polycrystalline diamond are shown in Figure 4. Ion-induced graphitization under irradiation with argon ions manifests itself in the RS spectra in the form of broadened D and G peaks. The diamond peak is also observed due to the optical transparency of a thin  $\sim 30\text{ nm}$  graphite-like layer. The intensity ratio  $I_D/I_G$  and the positions of the D and G peaks correspond to graphite with a high concentration of radiation damage [24].

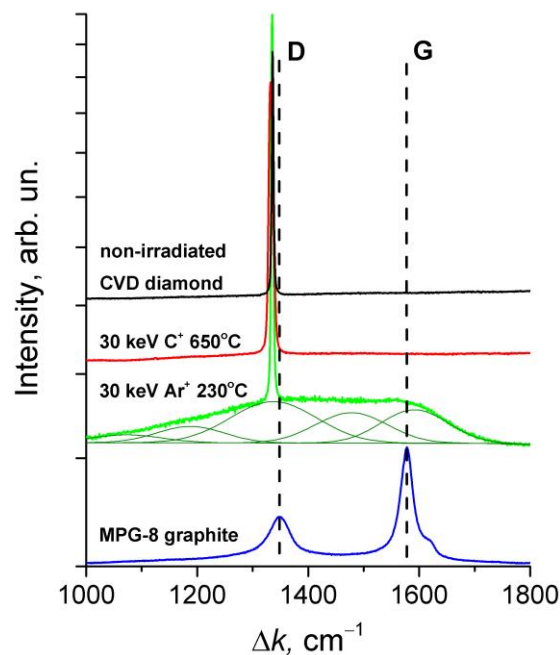


**Figure 4.** Raman spectra for chemical vapor deposition (CVD) diamond before and after irradiation by 30 keV  $\text{Ar}^+$  and  $\text{C}^+$  ions. Spectrum for polycrystalline graphite MPG-8 was measured for comparison. The Gaussian analyses of the spectrum are shown by thin lines for diamond irradiated with  $\text{Ar}^+$  ions.

The Raman spectrum after irradiation with carbon ions shows that synthesizing a diamond surface with a size of  $\sim 0.1 \mu\text{m}$  practically does not result in a difference from the Raman spectrum of the initial diamond. This indicates a good crystallinity of the synthesized diamond layer upon the implantation of carbon ions. Similar results were obtained for single crystal diamond [12].

#### 3.4. Conductivity of the Ion-Modified Layer

It is known that recrystallization during diamond annealing after ion implantation at temperatures  $< 60 \text{ }^\circ\text{C}$  occurs only at low irradiation fluences, which do not lead to a vacancy concentration of more than  $10^{22} \text{ cm}^{-3}$  [25]. The isochronous annealing of the implanted diamond with a final temperature  $T_a = 1200 \text{ }^\circ\text{C}$  leads to an almost initial structure. At high irradiation fluences, a disordered irradiated diamond layer undergoes an irreversible transition to graphite-like structures under annealing. The processes of the graphitization of thin layers in diamond under ion irradiation are of interest for the creation of conductors on the surface of diamond and various diamond–graphite heterostructures [26–28].

Due to the dielectric properties of diamond, the analysis of the conductivity of modified layers is a simple and effective method for assessing ion-induced structural changes. This is demonstrated by the dependences of the conductivity  $\sigma = (R_s \cdot t)^{-1}$  of the modified diamond layers on the irradiation and annealing temperatures shown in Figure 5. The dotted lines in the figure show the range of conductivity values typical for prepreps of synthetic graphites in the process of graphitization at  $T_a > 1000 \text{ }^\circ\text{C}$ . It can be seen that the conductivity of the irradiated-at- $30 \text{ }^\circ\text{C}$  diamond layer, comparable to that of graphitized carbon materials, begins at  $T_a > 300 \text{ }^\circ\text{C}$ . The increasing character of the  $\sigma(T_a)$  dependences suggests that an increase in  $T_a > 700 \text{ }^\circ\text{C}$  will lead to an even greater increase in the conductivity of the irradiated layer. It should be noted that at  $T_a \geq 1300 \text{ }^\circ\text{C}$ , the transformation of diamond into graphite begins. More efficient graphitization occurs with “hot” irradiation (Figure 5) (see [11]). A sharp increase in conductivity begins at a  $T$  of about  $150 \text{ }^\circ\text{C}$ ; then, after passing the maximum of about  $300 \text{ }^\circ\text{C}$ , a decrease in the conductivity is observed, which is small for irradiation with argon and significant for irradiation with carbon ions.

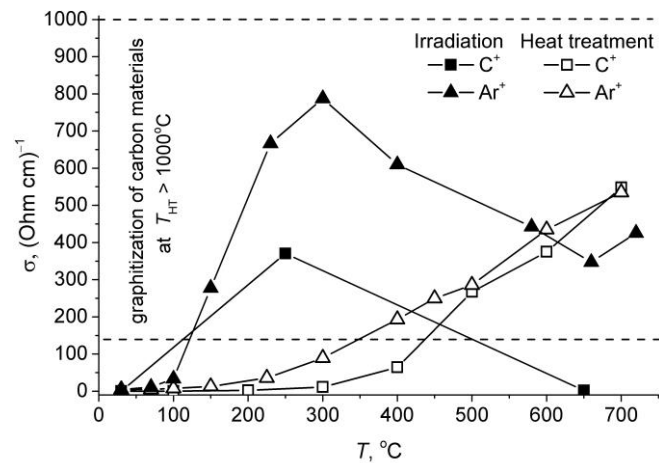


**Figure 5.** Dependences of the conductivity  $\sigma$  of the irradiated polycrystalline diamond layers on the irradiation temperature  $T$  and annealing  $T_a$ .

A decrease in conductivity at 400–600 °C is associated with the formation of nanocrystalline graphite, which has a lower conductivity [11,12]. It can be seen from the figure that a graphite-like layer can also be obtained by irradiating diamond with carbon ions at a temperature corresponding to the maximum conductivity of the modified layer. Thus, it can be assumed that irradiation with carbon ions makes it possible to process the diamond either with the formation of a graphite layer or with the growth of the diamond surface. Vacuum arc sources, which have successfully been used for both coating deposition [5–9] and for implantation [29], can be suitable generators of carbon ions.

#### 4. Conclusions

The graphitization and growth of diamond surfaces by the high-fluence ( $>10^{18}$  ion/cm<sup>2</sup>) irradiation with 30 keV argon and carbon ions of CVD diamond and the (111) face of HPHT diamond were experimentally studied.

To characterize the high-fluence ion irradiation, the depth distributions  $\nu(x)$  of the numbers of displacements per atom (dpa) were calculated using the SRIM code. Based on the calculated profiles of  $\nu(x)$ , the thickness of the modified surface layer was estimated for Ar<sup>+</sup> and C<sup>+</sup> ion irradiation. Unlike for irradiation for argon ions, for carbon ion irradiation, the thickness of the modified layer increased due to the implanted carbon ions.

SEM and AFM showed the removal of traces of mechanical polishing under Ar<sup>+</sup> and C<sup>+</sup> ion irradiation and the appearance of a stochastic microrelief. The roughnesses before and after the ion irradiation of the diamond surface are close—the root-mean-square roughness at a base length of 1  $\mu$ m is about 20 nm.

Raman spectroscopy before and after the CVD diamond irradiation showed the graphitization of the surface layer when irradiated with argon ions at the temperature of 230 °C and a diamond structure for the synthesized layer when irradiated with carbon ions at the temperature of 650 °C.

The measurement of the conductivity of the modified layer on diamond is a simple and effective method for determining the irradiation or annealing temperature to obtain a graphitized modified layer. Graphite conductivity is obtained at a diamond irradiation temperature of about 300 °C. Annealing a diamond irradiated at room temperature can also lead to a graphitized layer. The measurement of the electrical conductivity of irradiated CVD diamonds showed that the graphitization of the surface layer can also be obtained by irradiation with carbon ions.

**Author Contributions:** Conceptualization, S.N.G.; methodology, I.V.S.; validation, E.S.M.; investigation, A.M.B., V.A.K., M.A.O. and E.S.M.; writing—original draft preparation, A.M.B.; writing—review and editing, E.S.M. and M.A.O.; project administration, S.N.G. All authors have read and agreed to the published version of the manuscript.

**Funding:** This research was funded by the Ministry of Science and Higher Education of the Russian Federation, grant number 0707-2020-0025.

**Conflicts of Interest:** The authors declare no conflict of interest.

## Abbreviations

Symbol	Description
AFM	atomic force microscopy
CVD	chemical vapor deposition
G	graphitic carbon band
HPHT	high-pressure, high-temperature
D	disordered carbon band
ID/IG	ratio of the intensities (height) of D and G bands
SEM	scanning electron microscopy

## References

- Grigoriev, S.; Melnik, Y.; Metel, A. Broad fast neutral molecule beam sources for industrial-scale beam-assisted deposition. *Surf. Coat. Technol.* **2002**, *156*, 44–49. [[CrossRef](#)]
- Colligon, J.S.; Vishnyakov, V.; Valizadeh, R.; Donnelly, S.T.; Kumashiro, S. Study of nanocrystalline TiN/Si<sub>3</sub>N<sub>4</sub> thin films deposited using a dual ion beam method. *Thin Solid Film.* **2005**, *485*, 148–154. [[CrossRef](#)]
- Metel, A.; Bolbukov, V.; Volosova, M.; Grigoriev, S.; Melnik, Y. Source of metal atoms and fast gas molecules for coating deposition on complex shaped dielectric products. *Surf. Coat. Technol.* **2013**, *225*, 34–39. [[CrossRef](#)]
- Metel, A.; Bolbukov, V.; Volosova, M.; Grigoriev, S.; Melnik, Y. Equipment for deposition of thin metallic films bombarded by fast argon atoms. *Instruments Exp. Tech.* **2014**, *57*, 345–351. [[CrossRef](#)]
- Sobol', O.V.; Andreev, A.A.; Grigoriev, S.N.; Gorban', V.F.; Volosova, M.A.; Aleshin, S.V.; Stolbovoy, V.A. Physical characteristics, structure and stress state of vacuum-arc tin coating, deposition on the substrate when applying high-voltage pulse during the deposition. *Probl. At. Sci. Technol.* **2011**, *4*, 174–177.
- Grigoriev, S.N.; Sobol, O.V.; Beresnev, V.M.; Serdyuk, I.V.; Pogrebnyak, A.D.; Kolesnikov, D.A.; Nemchenko, U.S. Tribological characteristics of (TiZrHfVNBa)N coatings applied using the vacuum arc deposition method. *J. Frict. Wear* **2014**, *35*, 359–364. [[CrossRef](#)]
- Kuzin, V.V.; Grigor'ev, S.N.; Volosova, M.A. Effect of a tic coating on the stress-strain state of a plate of a high-density nitride ceramic under nonsteady thermoelastic conditions. *Refract. Ind. Ceram.* **2014**, *54*, 376–380. [[CrossRef](#)]
- Volosova, M.A.; Grigor'ev, S.N.; Kuzin, V.V. Effect of titanium nitride coating on stress structural inhomogeneity in oxide-carbide ceramic. Part 4. Action of heat flow. *Refract. Ind. Ceram.* **2015**, *56*, 91–96. [[CrossRef](#)]
- Kuzin, V.V.; Grigoriev, S.N.; Fedorov, M.Y. Role of the thermal factor in the wear mechanism of ceramic tools. Part 2: Microlevel. *J. Frict. Wear* **2015**, *36*, 40–44. [[CrossRef](#)]
- Nelson, R.S.; Hudson, J.A.; Mazey, D.J.; Piller, R.C. Diamond synthesis: Internal growth during C<sup>+</sup> ion implantation. *Proc. R. Soc. London Ser. A Math. Phys. Sci.* **1983**, *386*, 211–222. [[CrossRef](#)]
- Borisov, A.M.; Kazakov, V.A.; Mashkova, E.S.; Ovchinnikov, M.A. The regularities of high-fluence ion-induced graphitization of diamond. *Vacuum* **2018**, *148*, 195–200. [[CrossRef](#)]
- Borisov, A.M.; Kazakov, V.A.; Mashkova, E.S.; Ovchinnikov, M.A.; Pitirimova, E.A. On the dynamic annealing of ion-induced radiation damage in diamond under irradiation at elevated temperatures. *J. Surf. Investig. X-ray Synchrotron Neutron Tech.* **2019**, *13*, 306–313. [[CrossRef](#)]
- Borisov, A.M.; Kazakov, V.A.; Mashkova, E.S.; Ovchinnikov, M.A.; Palyanov, Y.N.; Popov, V.P.; Shmytkova, E.A. Optical and electrical properties of synthetic single-crystal diamond under high-fluence ion irradiation. *J. Surf. Investig. X-ray Synchrotron Neutron Tech.* **2017**, *11*, 619–624. [[CrossRef](#)]
- Borisov, A.M.; Kazakov, V.A.; Mashkova, E.S.; Ovchinnikov, M.A.; Shemukhin, A.A.; Sigalae, S.K. The conductivity of high-fluence noble gas ion irradiated CVD polycrystalline diamond. *Nucl. Instrum. Methods Phys. Res. B.* **2017**, *406*, 676–679. [[CrossRef](#)]

15. Andrianova, N.N.; Borisov, A.M.; Kazakov, V.A.; Mashkova, E.S.; Popov, V.P.; Palyanov, Y.N.; Risakhanov, R.N.; Sigalae, S.K. High-fluence ion-beam modification of a diamond surface at high temperature. *J. Surf. Investig. X-ray Synchrotron Neutron Tech.* **2015**, *9*, 346–349. [[CrossRef](#)]
16. Andrianova, N.N.; Borisov, A.M.; Kazakov, V.A.; Mashkova, E.S.; Palyanov, Y.N.; Pitirimova, E.A.; Popov, V.P.; Rizakhanov, R.N.; Sigalae, S.K. Graphitization of a diamond surface upon high-dose ion bombardment. *Bull. Russ. Acad. Sci. Phys.* **2016**, *80*, 156–160. [[CrossRef](#)]
17. Mashkova, E.S.; Molchanov, V.A. *Medium-Energy Ion Reflection from Solids*; Elsevier: Amsterdam, The Netherlands, 1985.
18. Ziegler, J.F.; Biersack, J.P. SRIM. 2013. Available online: [www.srim.org](http://www.srim.org) (accessed on 18 August 2019).
19. Ehrhart, P.; Schilling, W.; Ullmaier, H. Radiation damage in crystals. *Encycl. Appl. Phys.* **1996**, *15*, 429–457.
20. Roth, J. Chemical sputtering. In *Sputtering by Particle Bombardment II*; Behrisch, R., Ed.; Springer: Berlin/Heidelberg, Germany; New York, NY, USA; Tokyo, Japan, 1983; pp. 91–141.
21. Andrianova, N.N.; Borisov, A.M.; Mashkova, E.S.; Shemukhin, A.A.; Shulga, V.I.; Virgiliev, Y.S. Relief evolution of HOPG under high-fluence 30 keV argon ion irradiation. *Nucl. Instrum. Methods Phys. Res. B* **2015**, *354*, 146–150. [[CrossRef](#)]
22. Anikin, V.A.; Borisov, A.M.; Kazakov, V.A.; Mashkova, E.S.; Palyanov, Y.N.; Popov, V.P.; Shmytkova, E.A.; Sigalae, S.K. Diamond single crystal-surface modification under high-fluence ion irradiation. *J. Phys. Conf. Ser.* **2016**, *747*, 12025. [[CrossRef](#)]
23. Ferrari, A.C.; Robertson, J. Resonant Raman spectroscopy of disordered, amorphous, and diamondlike carbon. *Phys. Rev. B* **2001**, *64*, 75414. [[CrossRef](#)]
24. Niwase, K. Raman spectroscopy for quantitative analysis of point defects and defect clusters in irradiated graphite. *Int. J. Spectrosc.* **2012**, *2012*, 197609. [[CrossRef](#)]
25. Kalish, R. Doping diamond by ion-implantation. *Semicond. Semimet.* **2003**, *76*, 145–181. [[CrossRef](#)]
26. Popov, V.P.; Safronov, L.N.; Naumova, O.V.; Nikolaev, D.V.; Kupriyanov, I.N.; Palyanov, Y.N. Conductive layers in diamond formed by hydrogen ion implantation and annealing. *Nucl. Instrum. Methods Phys. Res. B* **2012**, *282*, 100–107. [[CrossRef](#)]
27. Philipp, P.; Bischoff, L.; Treske, U.; Schmidt, B.; Fiedler, J.; Hübner, R.; Klein, F.; Koitzsch, A.; Mühl, T. The origin of conductivity in ion-irradiated diamond-like carbon—Phase transformation and atomic ordering. *Carbon* **2014**, *80*, 677–690. [[CrossRef](#)]
28. Rubanov, S.; Suvorova, A.; Popov, V.P.; Kalinin, A.A.; Pal'yanov, Y.N. Fabrication of graphitic layers in diamond using FIB implantation and high pressure high temperature annealing. *Diam. Relat. Mater.* **2016**, *63*, 143–147. [[CrossRef](#)]
29. Brown, I.G. *The Physics and Technology of Ion Sources*; Lawrence Berkeley Laboratory, University of California: Berkeley, CA, USA, 1989.

**Publisher's Note:** MDPI stays neutral with regard to jurisdictional claims in published maps and institutional affiliations.



© 2020 by the authors. Licensee MDPI, Basel, Switzerland. This article is an open access article distributed under the terms and conditions of the Creative Commons Attribution (CC BY) license (<http://creativecommons.org/licenses/by/4.0/>).